To be submitted for publication

LBL-8503
Preprint

NUMERICAL SIMULATION OF VORTEX BREAKDOWN

Vincenza Del Prete

October 1978

Prepared for the U. S. Department of Energy
under Contract W-7405-ENG-48

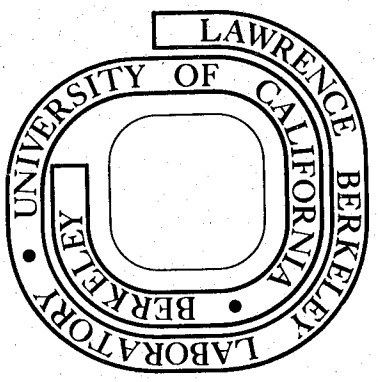

LBL-8503

NUMERICAL SIMULATION OF VORTEX BREAKDOWN

Vincenza Del Prete

University of California
Berkeley, California 94720

and

Università di Genova
Genova, Italy

October 1978

This work was partially supported by O.N.R. grant no. N0014-69-A-0200-1052 and by the Engineering, Mathematical, and Geosciences Division of the U.S. Department of Energy.

ABSTRACT

Vortex breakdown is simulated by a three dimensional Lagrangian method using vortex filaments. The filaments are approximated by vortex elements and their velocity is computed by a Biot-Savart type law of interaction. The numerical calculations show the development of an axisymmetric bubble with a recirculation zone and resemble in many respects the results obtained in the physical experiments on vortex breakdown.

Introduction

A vortex breakdown is an abrupt disturbance which occurs in some flows which have a region of concentrated vorticity. Such flow can be obtained by sending fluid through a tube and giving it swirl with a set of vanes at the inlet station. In most experiments the tube is slightly divergent in the direction of the flow. The region of concentrated vorticity is located around the axis of the tube and is called the vortex core. The basic flow is a steady streamwise vortex and outside the vortex core it is approximately irrotational. For reasons which have not been completely clarified, a stagnation point followed by a region of reversed flow may occur on the axis of the vortex. This may be followed by the loss of the coherent nature of the flow. This sequence of events is called a vortex breakdown. Changes in the conditions at the inlet station give different forms of the same phenomenon. Two forms predominate: namely the spiral and the "axisymmetric" bubble. We shall only discuss the latter case.

In all experiments the vortex breakdown is associated with an adverse pressure gradient in the vortex core, i.e., the pressure increases in the direction of the flow. This may be caused by a deceleration of the outer flow which, for example, may be due to the divergence of the tube. Thus the occurrence of the vortex breakdown depends on a balance between at least three parameters, the swirl of the flow, the divergence of the tube, and the adverse pressure gradient, see Hall (1972).

The phenomenon has been visualized by introducing dye at the center of the inlet station, see Sarpkaya (1971). One observes that the axial

filament suddenly expands in a nearly axisymmetric envelope. The bubble is closed at the upstream end, while at the rear it is continuously emptied and refilled from two different azimuthal directions. Physical experiments by Sarpkaya (1971) and Leibovitch (1978) have shown that the inner part of the bubble contains one or two recirculation zones which are created by the vortex rings trapped in the bubble.

Vortex breakdown is important from a practical point of view. It occurs in combustion problems and in aerodynamical problems. Its occurrence is desirable in gas turbine combustors, and it helps to dissipate vortices behind large aircraft.

Vortex breakdown has been the subject of many theoretical and numerical investigations. Roughly speaking, there are three theories, but none of them has received general acceptance. An extensive and comparative analysis has been carried out by Hall (1972) and Leibovitch (1978). In the first theory, due to Gartshore (1963), Hall (1972), and Mager (1972), vortex breakdown is interpreted as corresponding to the failure of the quasi-cylindrical approximation of the Navier-Stokes equations. The theory is analogous to boundary layer theory. In the second theory, due to Ludwig (1970), vortex breakdown is explained as a consequence of an instability of the flow to helical disturbances. Our numerical experiments are based on the third theory, the wave theory, and to the extent that they are successful they do support it. In the wave theory, vortex breakdown is interpreted as a standing wave. Following Benjamin (1962), an inviscid flow is called supercritical if waves can only propagate in the direction of the flow and subcritical if waves can also propagate in the upstream direction. A flow is called critical if standing waves are possible. This can be cast in mathematical terms. The

theory fails if the flow is viscous. On the other hand, according to Leibovitch (1978), all breakdowns for which velocity data exist are supercritical upstream and subcritical downstream. Our numerical experiments do not show dependence on this classification. This may be due to the limited resolution in our technique. We follow Squire (1960) and assume that vortex breakdown occurs when a perturbation can travel upstream from a downstream source of disturbance. This is confirmed by Sarpkaya's experiments (1971) which show that vortex breakdown is sensitive to changes in the downstream flow conditions. In this paper we simulate the vortex breakdown by using vortex filaments extending to infinity to represent the vortex core and vortex rings to represent the trapped wave in the bubble.

The plan of the paper is as follows: In section 2 we present the random vortex method due to Chorin (1973). In section 3 we extend the vortex method to three dimensions by using vortex filaments instead of point vortices. The main problem is the discretization of the filaments which extend to infinity. The difficulty is overcome by treating the parts of the filaments which are far from the perturbation as straight lines. The filaments near the perturbation are approximated by vortex elements. These are moved by the velocity field which is created by the filaments themselves. The velocity of each vortex element is computed by using a Biot-Savart type law of interaction between all the elements. To smooth out the velocity field due to nearby vortex elements, we modify the Biot-Savart law near the singularity. This is accomplished by using a cutoff.

In section 4 we use Mager's approximation of the experimentally observed velocity profiles to determine the distribution of vorticity at the inlet station. We approximate the distribution of vorticity by vortex filaments.

According to Leibovitch (1976), it is unlikely that the viscosity plays a significant role in the vortex breakdown. Thus we consider only the diffusion of vorticity in the radial direction and simulate the effect of the viscosity by displacing the vortex elements in the radial direction by using a random walk technique. Finally in section 5 we present the numerical experiments. These show the development of an axisymmetric bubble with a recirculation zone and resemble in many respects the pictures of vortex breakdown in some of the physical experiments due to Sarpkaya (1971).

2. The two-dimensional random vortex method

The vorticity equation for an incompressible, inviscid flow is

$$\xi_t + u\xi_x + v\xi_y = 0 \tag{1}$$

where $\underline{u} = (u,v)$ is the velocity field, $\xi = \text{curl } \underline{u}$ is the vorticity, and t is the time.

Since the flow is incompressible, the divergence of $\underline{u}$ is equal to zero, and u and v can be expressed in terms of the stream function ψ in the following way:

$$\Delta\psi = -\xi, \qquad u = \psi_y, \qquad v = -\psi_x \ . \tag{2}$$

A flow whose distribution of vorticity is zero everywhere and is κ at z_0 is called a potential vortex at z_0. The Green function for the Laplacian in the plane is $G(z) = -(2\pi)^{-1}\log|z|$ where $|z|^2 = x^2 + y^2$. The stream function for a potential vortex at z_0 is

$$\psi(z) = -\kappa \cdot (2\pi)^{-1}\log|z - z_0| \ . \tag{3}$$

Let ξ_0 be the initial distribution of vorticity. We partition the support of ξ_0 into nonoverlapping blobs B_j. It follows from Kelvin's circulation theorem that the integral $\kappa_j = \int_{B_j} \xi_0 dxdy$ is constant in time. At time $t = 0$ we approximate the vorticity function ξ_0 by $\xi = \sum_j \kappa_j \delta(z-z_j)$. Here $z_j = (x_j, y_j)$ is the center of gravity of B_j, and $\delta(z)$ is the delta function at the origin. The flow corresponding to ξ consists of a system of potential vortices. By using equations (2) and (3) we find that the stream function ψ and the velocity field (u,v) corresponding to ξ are

$$\psi_i = (2\pi)^{-1} \sum_j \kappa_j \log(z_i - z_j) \tag{4}$$

$$u_i = \frac{1}{2\pi} \sum_{j \neq i} \kappa_j \frac{y_i - y_j}{r_{ij}^2}, \qquad v_i = -\frac{1}{2\pi} \sum_{j \neq i} \kappa_j \frac{x_i - x_j}{r_{ij}^2}$$

for $i = 1,\ldots,N$. Here u, v and ψ are evaluated at z_i and $r_{ij}^2 = (x_i - x_j)^2 + (y_i - y_j)^2$. The motion of the point vortices is then described by

$$\dot{x}_i = u_i, \quad \dot{y}_i = v_i \tag{5}$$

for $i = 1,2,\ldots,N$. The velocity field can be arbitrarily large near a point vortex. As pointed out by Chorin and Bernard (1973), this is unphysical and leads to instabilities. Therefore we replace the stream function G for a potential vortex by a smoother function G_δ. The expressions for the velocity in (4) then become $u_i = \sum_{j \neq i} \kappa_j \partial_y G_\delta$ and $v_i = -\sum_{j \neq i} \kappa_j \partial_x G_\delta$, where the derivatives of G_δ are computed at $z_i - z_j$. This idea is due to Chorin (1973). His cutoff is $G_\delta(r) = (2\pi)^{-1}(1 - r/\delta - \log\delta)$ for $r < \delta$ and $G_\delta = G$

for $r > \delta$. Other cutoffs can be obtained by prescribing a smooth link at $r = \delta$, and a zero derivative at the origin. For a comparative analysis and a convergence proof, see Hald and Del Prete (1978).

We consider now a viscous flow. The Navier-Stokes equation for an incompressible viscous flow is

$$\xi_t = - (\underline{u} \cdot \underline{\nabla})\xi + R^{-1}\Delta\xi \ , \tag{6}$$

where R is the Reynolds number. The right-hand side of equation (6) is the sum of a nonlinear term and a linear diffusion term. To simulate the effect of the diffusion term we use random walks. We will describe the method briefly. Consider the heat equation

$$\xi_t = R^{-1}\Delta\xi \ , \quad \xi(x,y,t=0) = \xi_0 \ .$$

We represent ξ_0 as the sum of ξ_i where ξ_i are point masses at (x_i,y_i) Let Δt be the time step, and let x_i^n and y_i^n be the positions at time $t = n\cdot\Delta t$. We move the points according to

$$x_i^{n+1} = x_i^n + \eta_1 \qquad y_i^{n+1} = y_i^n + \eta_2 \ ,$$

where η_1 and η_2 are Gaussianly distributed random variables with zero mean and variance $2\cdot\Delta t/R$. Let $u_i^{n,\frac{1}{2}}$ and $v_i^{n,\frac{1}{2}}$ be the components of the velocity obtained by solving the equation of motion for the point vortices by the midpoint rule. Here the right-hand side of (5) is defined using the cutoff. By combining the midpoint rule with the random method, we obtain the following algorithm

$$x_i^{n+1} = x_i^n + \Delta t \cdot u^{n,\frac{1}{2}} + \eta_1$$

$$y_i^{n+1} = y_i^n + \Delta t \cdot v^{n,\frac{1}{2}} + \eta_2 \ .$$

The vorticity density generated by the motion of the vortices according to these laws will approximate the solution of (5), see Chorin (1973).

3. The three-dimensional vortex method

Let $\underline{u}$ and $\underline{\xi}$ be the velocity field and the distribution of vorticity for an incompressible flow. Then curl $\underline{u} = \underline{\xi}$ and div $\underline{u} = 0$. A solution of these equations is given by

$$\underline{u}(\underline{x}) = \int \nabla G(\underline{x} - \underline{x}') \times \underline{\xi}(\underline{x}') d\underline{x}' \ , \qquad (7)$$

see Batchelor (1967, p. 87). Here $G(\underline{x}) = (4\pi|x|)^{-1}$ is the Green function for the Laplacian in three dimensions. The remaining solutions of the differential equations can be obtained by adding a function of the form $\underline{u} = \text{grad } \phi$ to the right-hand side of (1). Here $\Delta\phi = 0$. Note that the vorticity in (7) depends upon the time t. Our interest is focused on two distributions of vorticity. In the first case $\underline{\xi} = (0,0,\Gamma(x^2+y^2))$ for $|z|$ large where $\Gamma = 0$ for $x^2+y^2 > 1$. In the second case $\underline{\xi}$ is the vector field corresponding to a vortex ring.

We consider now a vorticity distribution which is Γ on a line C and zero elsewhere. This is called a vortex filament of strength Γ. In each point of the curve the vorticity vector has the same direction as the tangent to the curve. For such a distribution of vorticity the formula (7) reduces to the line integral

$$\underline{u}(\underline{x}) = \frac{\Gamma}{4\pi} \int_C \frac{(\underline{x} - \underline{x}') \times d\underline{s}'}{|\underline{x} - \underline{x}'|^3} \tag{8}$$

If the flow is inviscid then the vortex filament is a material line, and its strength is constant in time. This follows from Helmholtz's theorem and Kelvin's theorem, see Batchelor (1967, pp. 274 and 273). To discretize the line integral we choose a sequence of points P_i on the curve. The piece of filament which lies between two nodes is called a vortex element. We approximate the right-hand side of equation (8) by

$$\underline{u}(\underline{P}) \simeq \frac{\Gamma}{4\pi} \sum_i \frac{(P - P_i)}{|P - P_i|^3} \times (P_{i+1} - P_i) .$$

Here we have approximated the vorticity unit vector by the secant. As in the two-dimensional case, we smooth out the velocity field by replacing the Green function G by a smoother function G_δ. The formula for the velocity $\underline{u}$ then becomes

$$\underline{u}(P) \simeq \Gamma \sum_i \nabla G_\delta(P - P_i) \times (P_{i+1} - P_i) \tag{9}$$

In our experiments we use $G_\delta(r) = (4\pi\delta)^{-1}[(r/\delta)^3 - 2(r/\delta)^2 + 2]$ for $r < \delta$ and $G_\delta = G$ for $r \geqslant \delta$. Thus G_δ is twice continuously differentiable with respect to r and the first derivative vanishes at the origin.

The physical experiment can be interpreted as a basic flow through the tube plus a perturbation caused by the vortex breakdown. The vorticity field corresponding to the basic flow is parallel to the z axis and extends to infinity. We will assume that far from the perturbation the vortex filaments are straight lines. We compute the contribution of the perturbed region by

the formula (9). For the contribution of a half line parallel to the z axis we use instead the formula

$$\underline{u}(P) = \frac{\Gamma}{\sigma^2}\left(1 - \frac{|z - z_0|}{\sqrt{(z - z_0)^2 + \sigma^2}}\right) \cdot (y,-x,0) \ , \qquad (10)$$

where x, y and z are the coordinates of the point P, and z_0 is the end point of the half line. Here σ is the distance from P to the straight line. Formula (10) can be found by evaluating the integral (8). If $z - z_0$ is bounded away from zero then the velocity $\underline{u}$ tends to zero. However, the velocity may become unbounded as the point P tends to the end point of the half line. This possibility does not occur in our experiments because $z - z_0$ is kept different from zero.

4. Simulation of the breakdown

To simulate the physical experiment we use the experimental data on the velocities at the inlet station. We follow Mager (1972), who approximates the observed velocity at the inlet station by

$$\begin{aligned} &u = 0 \ , \quad v = Vr(2 - r^2) \ , \quad w = \alpha + (1 - \alpha)r^2(6 - 8r + 3r^2) \ , \quad \text{for} \quad r > 1 \\ &u = 0 \ , \quad v = V/r \ , \quad w = 1 \ , \quad \text{for} \quad r < 1 \ . \end{aligned} \qquad (11)$$

This corresponds to a zero vorticity outside the cylinder $x^2 + y^2 < 1$. The expression for the vorticity inside the cylinder is given in cartesian

coordinates by

$$\xi_x = 12V(\alpha-1)(1-r^2)x/r \qquad \xi_y = 12V(\alpha-1)(1-r^2)y/r \qquad \xi_z = 4V(1-r^2) \ .$$

Note the smooth transition to the irrotational flow at $r = 1$. The Reynolds number for the above problem is $R = u_\infty r_c/\nu$. Here u_∞ is the free stream axial velocity of the fluid, ν the viscosity, and r_c is the radial location at which the swirl velocity is largest.

The approximations (11) have been obtained after a scaling. Specifically all lengths have been divided by r_c and the velocities by u. The velocity depends upon two parameters V and α, both positive. Here V is the swirl velocity at $r = 1$. The values of α greater or less than one yield jet-like or wake-like velocity profiles. In our experiment $\alpha = 1$, i.e., we have uniform axial flow. The distribution of vorticity is

$$\xi_x = 0 \ , \qquad \xi_y = 0 \ , \qquad \xi_z = 4 \cdot V \cdot (1 - r^2) \tag{12}$$

for $r \leqslant 1$ and zero for $r > 1$.

In the wave theory the vortex breakdown is interpreted as a standing wave. In our experiments the flow consists of a basic flow and a perturbation. This is caused by the vortex rings which we use to simulate the standing wave. The basic flow is a two-dimensional flow which corresponds to the distribution of vorticity (12), plus a translation. It is therefore natural first to discretize the problem as a two-dimensional problem and then extend the discretization to three dimensions.

Let $\xi_0 = \xi_z$. As in section 2, we approximate the vorticity ξ_0 by a sum of delta functions $\sum_j \kappa_j \delta(z - z_j)$. We partition the unit circle into

blobs B_j by dividing it into annuli A_n, $n = 0,1,\ldots,M$, such that area $(A_n) = n \cdot$ area (A_0), see Figure 1. At the same time we cut each annulus into M_0 slices. This gives a partition into $N = (1+M) \cdot M_0$ blobs. It is our experience that to simulate the vortex breakdown one needs many filaments close to the axis. We consider now the straight lines through the points z_j and parallel to the z axis. These lines are vortex filaments with strength κ_j. To investigate the behavior of the axial filament in the physical experiment we shift all the filaments in A_0 onto the z axis.

To compute the contribution of a filament to the velocity of a node, we divide the cylinder into five regions by the planes $z = \pm h$ and $z = \pm 3h$. The parameter h is chosen so large that the perturbation takes place in the region $|z| \leqslant h$. We call this region the main tube. The part of the filaments between $-3h$ and $3h$ is discretized with nodes, while the remaining parts are treated as straight lines. The reason for this approach is that the velocity field due to a half-infinite straight line has a singularity near the end point.

We will now discuss in detail how to calculate the contribution to the velocity at a node Q_k in the main tube from a filament D extending to infinity. Let P_j be the nodes on D and denote the first and last node in the main tube by P_n and P_m. Let μ be the maximum of $k-n$ and $k-m$. We compute the contributions from the vortex elements $k-\mu$ to $k+\mu$ by using formula (9). The velocity contributions from the remaining parts of the filament is computed by formula (10).

We mention that to obtain an exact two-dimensional flow the velocity field should be calculated by always taking the same number of vortex elements above and below the node. This technique is useful for debugging the

program. We do not recommend it in general because it is too expensive.

We will now discuss how to compute the effect of the rings. Here is a very simple method. Assume that the nodes of each ring are in a plane orthogonal to the axis. In each node the direction of the vorticity is given by the tangent to the circle orthogonal to the axis having center on the axis and passing through the node. This method is only accurate at the beginning. At later times the nodes do not lie in the same plane. A more sophisticated method is the following: we interpolate the nodes on a ring by a periodic second-order spline. The direction of the vorticity at a node is given by the tangent to this curve in space. The method is only well defined if the number of nodes of each ring is odd. Note that a similar technique could be used also to compute the vorticity field for the infinite filaments, but this would increase the cost of the computation.

The distribution of vorticity at later times is given by the positions of the filaments. We will now discuss how to update the position of the nodes. The position of a node P in the main tube at time $t+\Delta t$ is obtained by integrating $\dot{P} = \underline{u}(P,t) + (0,0,1)$ by the midpoint rule. Here $\underline{u}$ is the velocity computed by adding the contributions from the rings and the filaments extending to infinity. The vector $(0,0,1)$ is the scaled free stream axial velocity. The remaining part of the filaments are moved as straight lines parallel to the axis. We treat the upstream and downstream parts differently. The position of the downstream filament is given by the last node in the main tube. The upstream filament is moved by the velocity field created by the vorticity at the inlet station.

An alternative way of calculating the velocities at the inlet station is to use the three-dimensional vortex method for the basic flow. Since

the basic flow consists of a two-dimensional flow plus a translation, it is sufficient to calculate the velocities in the x and y directions for all nodes in a plane orthogonal to the z axis. This is equivalent to using a two-dimensional vortex method with a complicated cutoff.

To take the viscosity into account, we modify the random walk method for the two-dimensional flow. We assume the vorticity diffuses radially outward from the axis and neglect the diffusion in the other directions. Since the flow is approximately two-dimensional far from the perturbation, we displace all nodes on each filament (randomly) by the same amount. According to Leibovitch, it is unlikely that viscosity plays a significant role in the vortex breakdown, and our numerical experiments confirm this.

We remark that the filaments undergo local stretching. If the distance between two nodes becomes too large, then we introduce a new node. This is placed at the middle of the of the segment between the two nodes.

Finally, we mention that when a node leaves the downstream end of the main tube then we introduce a new node upstream. Otherwise the part of the filament which is approximated by a straight line gets too close to the perturbation.

5. Numerical experiments

In this section we give the values of the parameters in the actual experiments. To partition the support of the vorticity at the inlet station we take $M_0 = 5$ and $M = 22$. This gives 115 filaments, but for economical reasons we take only the 30 filaments closest to the axis. Thus the vorticity vanishes for $r > .21$. The numerical experiments are not substantially

changed by adding more filaments. Initially we take 30 nodes on each filament with 10 nodes in the main tube. Let $h = 2/3$ and let α be the distance between the nodes at $t = 0$. If the distance between two nodes becomes larger than $11/8 \cdot \alpha$, we then introduce a new node. Smaller values of this parameter do not improve the results.

To simulate the standing wave we have used two vortex rings with strength $\gamma = -.5$ and radii .13 and .1. At time $t = 0$ they are located at $z = 0$ and $z = .03$. The value of γ has been chosen by experiments. If $|\gamma| < 0.5$ then the rings are carried downstream by the flow, whereas the rings travel upstream if $|\gamma| > .5$. Experiments with more than two rings have been unsuccessful because the rings separate in groups.

To calculate the velocity we use the cutoff described in section 3. After some experimentation we have chosen the cutoff length $\delta = .1$. However, for the nodes of the rings we use $\delta = .03$ when computing the contribution from the vortex elements of the rings. Otherwise the velocities of the rings become too small. Finally, we have solved the differential equation by the midpoint rule with $\Delta t = .05$ and used the Reynolds number $R = 5000$.

In Figure 2 we show the evolution of the breakdown up to time $T = .45$. We have plotted the z coordinate of the nodes versus the distance $\sqrt{x^2 + y^2}$ to the z axis. The filaments in Figure 2 are initially on the same azimuthal plane. Since the filaments from other planes give approximately the same profiles, we have an axisymmetric bubble. We observe that the bubble does not appear suddenly, and the swelling begins with the central filament. This is in agreement with the experiments by Sarpkaya (1971). Observe that only some of the filaments go around the vortex ring and that the filaments closest to the axis have been stretched most at time $T = .45$. About 28 new

nodes have been added in the main tube. The kink at the upstream end of the bubble and the spiraling of this filament around the bubble closely resemble one of the experiments by Sarpkaya (1971, Figure 5).

According to Leibovitch (1978), there should be two recirculation cells of opposite vorticity inside the bubble. In our experiments there is only one recirculation cell. We have been unable to reproduce Leibovitch's result numerically.

It has been observed by Sarpkaya (1971) that the vortex rings are inclined. We have not been able to see this, possibly because our partition of the support of the vorticity at the inlet station is too crude.

The kink at the rear end of the bubble at time $t = .45$ is interesting. It resembles the beginning of the tail in Figure 6 of Sarpkaya (1971). He reports that during the period of growth there is no tail. We believe that the resolution of our method is insufficient to reproduce the details of the tail. Thus the kink might be a numerical artifact.

Finally, we mention that some filaments close to the axis have segments with negative axial velocity. We have indicated these segments by minus signs.

Acknowledgments

The author thanks Alexandre J. Chorin and Ole H. Hald for helpful discussions. The problem was suggested by Alexandre J. Chorin. Ole H. Hald has provided a detailed criticism of a preliminary version of the paper. This paper was written while the author was visiting the University of California, Berkeley, with a fellowship from the Consiglio Nazionale delle Ricerche. The numerical calculations were carried out at the Lawrence Berkeley Laboratory

and partially supported by O.N.R. grant no. N0014-69-A-0200-1052 and by the Engineering, Mathematical, and Geosciences Division of the U.S. Department of Energy.

References

Batchelor, G. K. 1967. An introduction to fluid dynamics. Cambridge University Press.

Benjamin, T. B. 1962. Theory of the vortex breakdown phenomenon. J. Fluid Mech. 14: 593-629.

Chorin, A. J. 1973. Numerical study of slightly viscous flow. J. Fluid Mech. 57: 785-796.

Chorin, A. J. & Bernard, P. S. 1973. Discretization of a vortex sheet with an example of roll up. J. Computational Phys. 13: 423-429.

Gartshore, I. S. 1963. Some numerical solutions for the viscous core of an irrotational vortex. NRC Con. Aero Rep. LR-378.

Hald, O. & Del Prete, V. 1978. Convergence of vortex methods for Euler's equations. Math. Comp. 32: 791-809.

Hall, M. G. 1972. Vortex breakdown. Ann. Rev. Fluid Mech. 4: 195-218.

Leibovitch, S. 1976. Vortex breakdown: experiment and theory. Cornell University, College of Engineering Energy Project, Rep. EPR-76-8.

Leibovitch, S. 1978. The structure of the vortex breakdown. Ann. Rev. Fluid Mech. 10: 221-246.

Ludwig, H. 1970. Vortex breakdown. Dtsh Luft Raumfahrt, Rep. 70-40.

Mager, A. 1972. Dissipation and breakdown of a wing-tip vortex. J. Fluid Mech. 55: 609-628.

Sarpkaya, T. 1971. On stationary and travelling vortex breakdowns. J. Fluid Mech. 45: 545-559.

Squire, H. B. 1960. Analysis of the "vortex breakdown" phenomenon. Part 1. Aero Dept., Imperial Coll. London, Rep. 102.

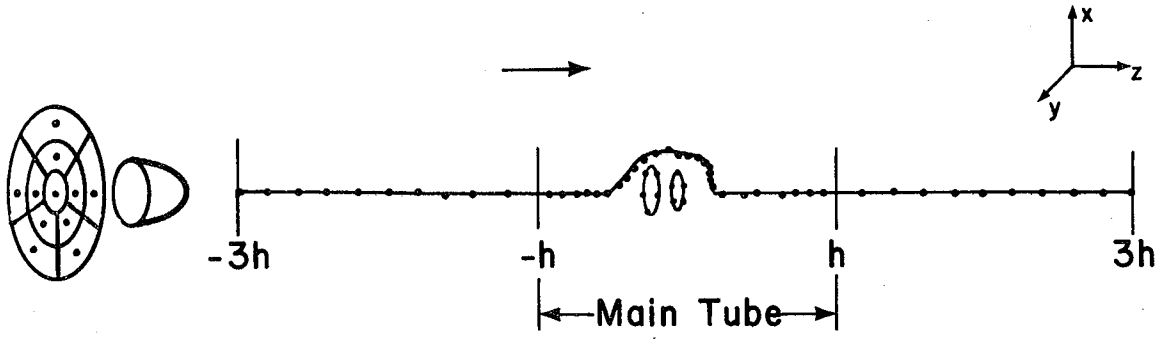

XBL 791-7

Fig. 1

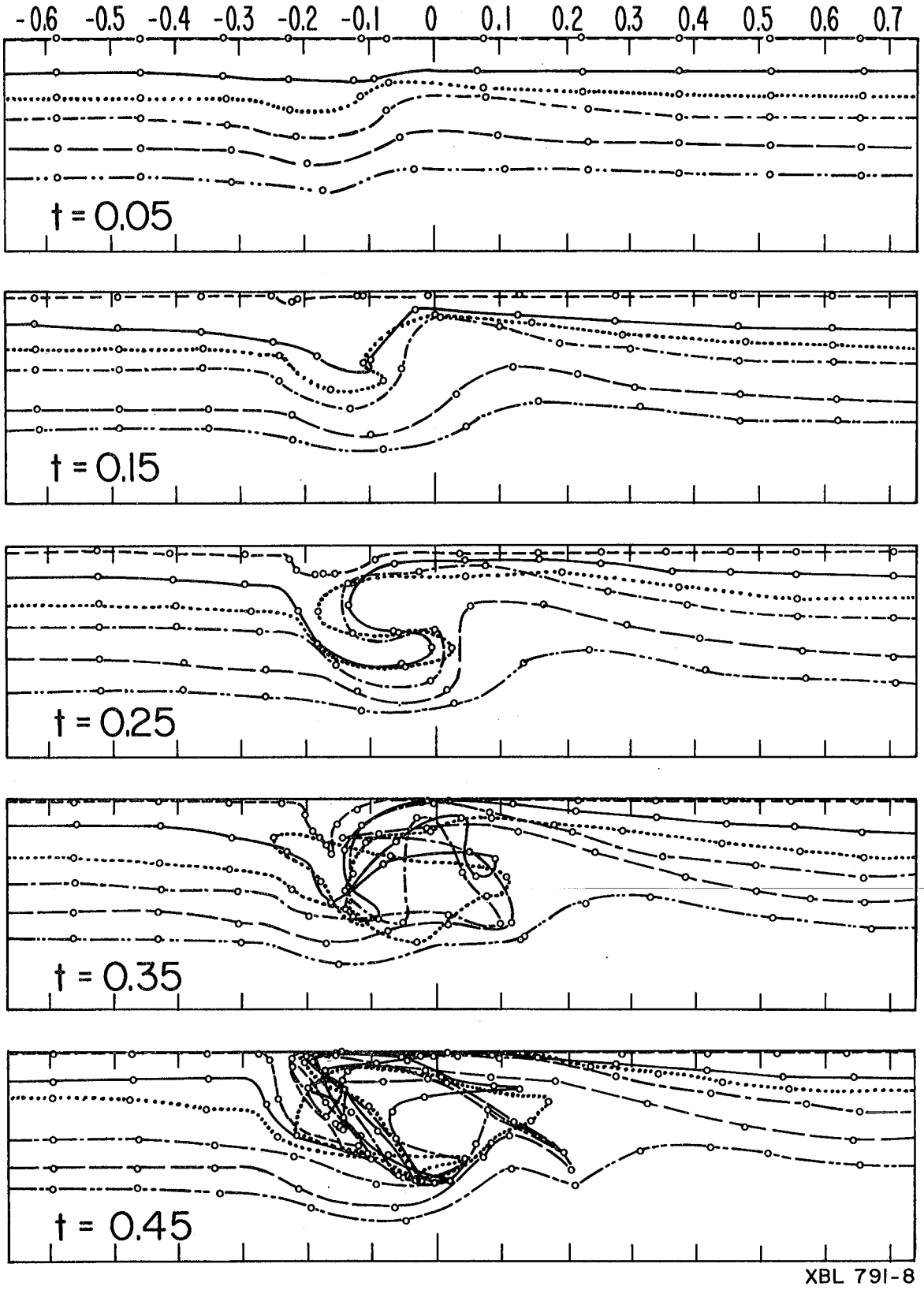
-0.6 -0.5 -0.4 -0.3 -0.2 -0.1 0 0.1 0.2 0.3 0.4 0.5 0.6 0.7
t = 0.05
t = 0.15
t = 0.25
t = 0.35
t = 0.45
XBL 791-8

Fig. 2

This report was done with support from the Department of Energy. Any conclusions or opinions expressed in this report represent solely those of the author(s) and not necessarily those of The Regents of the University of California, the Lawrence Berkeley Laboratory or the Department of Energy.

TECHNICAL INFORMATION DEPARTMENT
LAWRENCE BERKELEY LABORATORY
UNIVERSITY OF CALIFORNIA
BERKELEY, CALIFORNIA 94720